Published in final edited form as:
Neuroimage. 2012 September ; 62(3): . doi:10.1016/j.neuroimage.2012.06.008.

Atypical Lexicosemantic Function of Extrastriate Cortex in Autism Spectrum Disorder: Evidence from Functional and Effective Connectivity

Mark D. Shen[1,2], **Patricia Shih**[1,3], **Birgit Öttl**[1,4], **Brandon Keehn**[1,5,6], **Kelly M. Leyden**[1], **Michael S. Gaffrey**[1,7], and **Ralph-Axel Müller**[1]

[1] Brain Development Imaging Laboratory, Department of Psychology, San Diego State University, San Diego, CA, United States

[2]M.I.N.D. Institute, University of California, Davis, Davis, CA, United States

[3] Department of Neuroscience, Brown University, Providence, RI

[4]Department of Psychology, University of Tübingen, Germany

[5]Joint Doctoral Program in Language and Communicative Disorders, San Diego State University and University of California, San Diego, San Diego, CA, United States

[6]Children's Hospital, Harvard Medical School, Boston, MA, United States

[7]Department of Psychiatry, Washington University School of Medicine, St. Louis, MO, United States

Abstract

Previous studies have suggested atypically enhanced activity of visual cortex during language processing in autism spectrum disorder (ASD). However, it remains unclear whether visual cortical participation reflects isolated processing within posterior regions or functional cooperation with distal brain regions, such as left inferior frontal gyrus (LIFG). We addressed this question using functional connectivity MRI (fcMRI) and structural equation modeling in 14 adolescents and adults with ASD and 14 matched typically developing (TD) participants. Data were analyzed to isolate low-frequency intrinsic fluctuations, by regressing out effects of a semantic decision task. For a right extrastriate seed derived from the strongest cluster of atypical activation in the ASD group, widespread effects of increased connectivity in prefrontal and medial frontal lobes bilaterally were observed for the ASD group, compared to the TD group. A second analysis for a seed in LIFG, derived from pooled activation effects in both groups, also yielded widespread effects of overconnectivity in the ASD group, especially in temporal lobes. Structural equation modeling showed that whereas right extrastriate cortex did not impact function of language regions (left and right IFG, left middle temporal gyrus) in the TD model, it was an integral part of a language circuit in the ASD group. These results suggest that atypical extrastriate activation during language processing in ASD reflects integrative (not isolated) processing. Furthermore, our findings are inconsistent with previous reports of functional underconnectivity in ASD, probably related to removal of task effects required to isolate intrinsic low-frequency fluctuations.

Corresponding Author: Ralph-Axel Müller, Department of Psychology, San Diego State University, 6363 Alvarado Ct., Suite 200, San Diego, CA 92120 Tel.: 1-619-594-5276 Fax: 1-619-594-8707 amueller@sciences.sdsu.edu.

Keywords

Lexical; semantic; visual; functional connectivity; structural equation modeling; autism

Autism spectrum disorder (ASD) is a sociocommunicative disorder that is often characterized by delayed language development. Language abilities in ASD, however, vary greatly, from complete absence to apparently normal or even superior levels (Lord et al., 2004). Even among verbal children and adolescents with ASD who reach overall normal language levels, an uneven profile can be observed, with relatively unaffected phonological and morphosyntactic abilities being accompanied by lexicosemantic abnormalities (Boucher, 2012; Groen et al., 2008). Word production in children with ASD tends to be idiosyncratic or less prototypical than in TD children (Dunn et al., 1996), and naming has been found to be atypically fast for low-frequency words (Walenski et al., 2008). Individuals with ASD often commit semantic violations and have trouble processing semantic associations between words (Tager-Flusberg et al., 2005). Typically developing (TD) individuals show facilitation effects for semantic associations, identifying target words more quickly when primed with a word that is semantically related, whereas such facilitation effect has been reported absent in children and adults with ASD (Kamio et al., 2007). Moreover, semantic association performance in ASD has been found to correlate with nonverbal, rather than verbal, cognitive ability (Toichi and Kamio, 2001), suggesting atypical reliance on nonverbal cognitive processing in ASD. Semantic priming effects in ASD are significantly moderated by primer modality, with greater performance for priming with pictures than with words (Kamio and Toichi, 2000), further indicating a potentially enhanced role of visual processing in lexicosemantic representations in ASD.

As supported by a recent meta-analysis (Samson et al., 2011), atypically enhanced participation of extrastriate cortex has been observed in a number of fMRI studies of sentence comprehension (Kana et al., 2006), naming to definition (Knaus et al., 2008), and verbal working memory (Koshino et al., 2005). In a precursor study to the present investigation, Gaffrey et al. (2007) used a semantic decision task, in which participants decided whether visually presented words belonged to a target category (Tools, Colors, Feelings). Adolescents and adults with ASD made more errors than TD controls. The main imaging finding was atypical activation of extrastriate visual cortex (Brodmann areas [BAs] 18 and 19) in the ASD group. Previous studies thus suggest greater use of visual components during word-related task performance in ASD, which may however represent less efficient lexicosemantic processing.

While a number of studies have found atypically increased activity in the extrastriate cortex in ASD, the functional significance of these activations remains uncertain. Samson et al. (2011) suggest that such activity may reflect enhanced perceptual processing (Mottron et al., 2006). However, based on activation studies alone, it remains unclear whether atypical visual cortical activity reflects isolated, local processing or cooperation with other regions involved in semantic processing. We therefore used functional connectivity MRI (fcMRI) to characterize the role of atypical activity in the extrastriate cortex by examining intrinsic connectivity. As first observed by Biswal and colleagues (1995), low-frequency BOLD fluctuations (< 0.1Hz) show strong correlations within many functional networks (Beckmann et al., 2005; Fox and Raichle, 2007; Van Dijk et al., 2010), including motor (Jiang et al., 2004), auditory and visual (Cordes et al., 2001), and language networks (Hampson et al., 2002). These low-frequency oscillations, which are contained in and can be isolated from data acquired during task performance (Fair et al., 2007), can map out intrinsic connectivity networks (Van Dijk et al., 2010), which show overall good correspondence with anatomical networks as detected by diffusion tensor imaging (Honey et al., 2009). We

further applied structural equation modeling (SEM) to examine effective connectivity, i.e., the influence of a brain region over another (Büchel, 1997; Bullmore and Sporns, 2009; McIntosh and Gonzalez-Lima, 1994; Penny et al., 2004). Exploratory, data-driven SEM was performed to examine the directionality and connection strength between extrastriate and other cortical regions participating in lexicosemantic processing, such as left inferior frontal gyrus (LIFG).

The main objective of our study was to investigate whether extrastriate activity in ASD is merely a reflection of local processing bias (Dakin and Frith, 2005), which would be associated with limited connectivity to other regions; or conversely, whether extrastriate cortex cooperates with typical sites of lexical semantic activation, particularly LIFG.

Materials and Methods

Participants

Participants were 14 male adolescents and adults diagnosed with ASD (including ten from an earlier study by Gaffrey et al., 2007), individually matched with 14 TD participants on age, gender, handedness, and nonverbal IQ (Table 1). The ASD group included eight participants with autistic disorder, three participants with Asperger's disorder, and three participants with pervasive developmental disorder-not otherwise specified (PDD-NOS), assigned according to diagnostic criteria of the DSM-IV (American Psychiatric Association, 2000), Autism Diagnostic Interview-Revised (Lord et al., 1994), and the Autism Diagnostic Observation Schedule (Lord et al., 2000). All participants had full scale IQs above 80 on the Wechsler Abbreviated Scale of Intelligence (Wechsler, 1999). No individuals with any other diagnosable medical condition (e.g. Fragile X, tuberous sclerosis, epilepsy) were included in the study. The experimental protocol was approved by the Institutional Review Boards of San Diego State University and the University of California, San Diego.

Experimental tasks

As originally described by Gaffrey et al. (2007), participants indicated by button press whether a visually presented word belonged to a target category (Tools, Colors, Feelings). Each experimental block began with a target category (e.g., “TOOL?”) presented for 3.7 seconds. This was followed by 11 trials (2.5 s each), including eight target words (e.g., “HAMMER”) requiring a “yes” response, and three non-target words (e.g., “SOCCER”) requiring a “no” response. Each experimental block lasted 31.2 seconds, alternating with a perceptual control task. Each semantic category was presented twice per run. In the control task, participants indicated whether a target letter (“LETTER K?”) was present in a non-word letter string (e.g., “WKLNRT”). The control task had been calibrated in pilot studies (Gaffrey et al., unpublished data) to match the experimental task on task difficulty and visual complexity. Each control block began with the target letter prompt presented for 3.3 seconds, followed by five target (letter present) and two non-target (letter absent) trials presented for 2.5 seconds each. Each control block lasted 20.8 seconds. In both conditions, target and non-target stimuli were presented in pseudo-randomized order. Assignment of left/right buttons for yes/no responses was counterbalanced across participants. Each participant completed two runs, and no stimulus was repeated within the experiment.

MRI data acquisition

Imaging data were collected on a 1.5 Tesla Siemens Symphony MR scanner (Erlangen, Germany) at the University of California, San Diego. For each participant, 228 whole-brain T2*-weighted volumes (114 per run) were acquired using a single-shot gradient-recalled echo-planar imaging sequence, each containing 28 sequentially acquired axial slices (5 mm slice thickness; in-plane resolution 4 mm^2; TR 2600 ms; TE 36 ms; flip angle 90°; field of

view [FOV] 256 mm; matrix 64 × 64). A high-resolution structural scan was also acquired for anatomical localization and overlay of statistical maps (180 slices; resolution 1 mm^3; TR 11.08 ms; TE 4.3 ms; flip angle 45°; FOV 256 mm; matrix 256 × 256).

FMRI analysis

All analyses were performed using Analysis of Functional NeuroImages {AFNI; afni.nimh.nih.gov/afni). The first three time points of each functional run were discarded due to signal instability. Image preprocessing included head motion correction, 3D volume registration to the structural image, spatial smoothing with an 8 mm FWHM Gaussian kernel, and spatial normalization to the 'Colin' N27 template in Talairach space. The two functional runs for each participant were concatenated into a single time series. A deconvolution analysis (AFNI, 3dDeconvolve) was used to assess the hemodynamic changes associated with the experimental compared to the control condition, using a smoothed and shifted boxcar model of the alternating experimental and control blocks as hemodynamic model. Main effects of task were examined by means of general linear tests (Holmes et al., 1997). Fit coefficients for each voxel were entered into one-sample t-tests for within-group analyses and two-sample independent t-tests for group comparisons. To adjust for multiple comparisons, cluster size significance was determined by Monte-Carlo alpha simulations (Forman et al., 1995) for a corrected significance threshold of $p < 0.05$.

Functional connectivity analysis

Activation results were used to derive the regions of interest (ROIs) used as seeds for functional connectivity analysis. As expected from previous results in a smaller sample (Gaffrey et al., 2007), we found a significant activation cluster in extrastriate visual cortex in the ASD group, which was used as ROI. Pre-processing for functional connectivity analysis included removing the linear trend and applying a low-pass filter at 0.1 Hz to isolate low-frequency components of the BOLD signal, based on evidence indicating that BOLD synchronization reflecting intrinsic network connectivity is strongest in the low-frequency domain below 0.1 Hz (Cordes et al., 2000). The low-pass filter also served to reduce higher frequency noise, such as cardiac and respiratory effects. For each participant, a mean time series was extracted from the extrastriate ROI and was correlated with all other voxels in the brain. In order to remove effects of head motion, six motion time series (three rotational and three translational parameters) were included as orthogonal task regressors. To remove task-driven activation effects, a model of task-control cycles, based on the HRF estimate derived from deconvolution analysis of activation effects, was also used as an orthogonal regressor. Single-subject level connectivity maps for the extrastriate seed were entered into one-sample t-tests for within-group analyses and two-sample independent t-tests for group comparison. Cluster correction (Forman et al., 1995) was again performed for a corrected significance threshold of $p < 0.05$.

Structural equation modelling of effective connectivity

SEM was performed to further explore the strength and directionality of connections between cortical regions involved in semantic processing. ROIs were selected from activation clusters identified in a pooled analysis combining both groups and were informed by findings from prior studies of semantic processing in healthy adults (Hampson et al., 2002) and in ASD (Gaffrey et al., 2007). Four regions of interest were included in the model: left inferior frontal gyrus (LIFG), homotopic right inferior frontal gyrus (RIFG), left middle temporal gyrus (LMTG), and right extrastriate cortex (RESC). ROIs were generated to contain 228 voxels (1824μl) each by thresholding the activation map separately for each cluster.

SEM was applied as implemented in AFNI 1dSEM (Chen, 2007; Alvarez et al., 2008). To explore the effect of RESC on the semantic network in ASD, the current study applied a data-driven SEM approach that did not exclude any anatomically valid paths *a priori* (Chaminade, 2003; James et al., 2009; Zhuang et al., 2005). The automated *forest growth* algorithm searches through all possible models in order to find the optimal model that fits each group's data (Chen, 2007). Model search was therefore performed, resulting in separate models for each group. The time series of each ROI was preprocessed using the identical procedure as for the fcMRI analysis (linear trends removed, motion regressed, task regressed, low-pass filtered), then concatenated across subjects within each group, and entered into 1dSEM as a fixed effects analysis. The lowest cost function for both groups was observed with a fixed residual variance set to 80% of the total variance (Gonçalves, 2001; McIntosh and Gonzalez-Lima, 1994). The optimal model for each group was then applied on the subject level to test individual model fit, and mean path coefficients within each group were tested for significant differences from zero.

In order to arrive at optimal fit, the models generated for each group were iteratively evaluated to maximize both fit and parsimony according to several measures of model fit (de Marco et al. 2009). The χ^2 statistic tests whether an observed model is significantly different from the fully saturated model (i.e. every possible outcome). The Parsimonious Fit Index (PFI) penalizes 'overfitting' of the model (defining too many paths) with values nearest to 1 indicating the best-fitting model (Bullmore et al., 2000). The root mean square error of approximation (RMSEA) is a parsimony-adjusted, population-based fit index that is insensitive to sample size and adjusts model fit by weighting indices of fit by the number of parameters being estimated, with values nearest to 0 indicating the best-fitting model (Steiger, 1990; Browne and Cudeck, 1993; de Marco et al. 2009). The Comparative Fit Index (CFI) is an incremental fit index that compares a series of models, starting with a baseline null model, and incrementally adds paths until a target model achieves a CFI value closest to 1, representing the best-fitting model (Bentler, 1990; Alvarez et al. 2008). The forest growth algorithm implemented in AFNI 1dSEM (Chen, 2007) is an exploratory, data-driven approach that iteratively compares all possible models against each other and derives the best model according to the above fit indices (Chen, 2007; http://afni.nimh.nih.gov/sscc/gangc/PathAna.html).

Results

Behavioral data

For accuracy, there was a significant interaction of group by condition [$F_{(3,46)} = 4.59$, $p < 0.05$]. For the semantic decision task, there was a significant between-group difference [$F_{(1,23)} = 9.07$, $p < 0.01$], with lower accuracy in the ASD [M (SD) = 79.7% (9.9)] than in the TD group [M (SD) = 89.6% (4.9)]. For the perceptual control task, both groups were equally accurate at detecting the target letter [ASD: M (SD) = 94.2% (4.5); TD: M (SD) = 94.0% (3.9); $F_{(1,23)} = 0.029$, $p = 0.87$]. For response times, no significant group difference was found for semantic decision [$F_{(1,23)} = 4.10$, $p = 0.06$]. However, for the control task response times were significantly longer in the ASD [M (SD) = 899.3ms (94.3)] compared to the TD group [M (SD) = 797.6ms (50.6); $F_{(1,14)} = 7.87$, $p < 0.014$].

Given the wide age range in both ASD and TD groups, a correlation analysis was conducted to investigate any relationship between age and behavioral performance. No significant correlations were found between age and task accuracy or reaction time in either group (all correlations: $p > 0.45$).

fMRI activation

Both groups showed robust activation in LIFG for semantic decision (Table 2). In the TD group, an extensive cluster was found in Brodmann areas (BAs) 44 and 45 of left inferior frontal gyrus (Fig. 1A), with additional clusters in left middle frontal gyrus and supplemental motor area. Subcortical clusters were observed for the TD group in left caudate nucleus and right cerebellum. Inverse effects (greater BOLD signal for control compared to semantic decision task) occurred bilaterally in parieto-occipital cortices, with additional smaller clusters in precentral gyrus bilaterally, left cingulate cortex (BA 31), and left middle frontal gyrus (BA 9).

In the ASD group, left inferior frontal activation was less extensive than in the TD group (Fig. 1A). However, direct between-group comparison did not reveal any significant differences in this region. The ASD group also showed extensive activation in right extrastriate visual cortex (BAs 17, 18), whereas in the TD group only a small cluster was found in area 17. A large cluster in the right cuneus was used as seed ROI for functional connectivity analysis. No significant inverse effects (control > semantic condition) were detected in the ASD group.

Given the diagnostic heterogeneity of our ASD sample, an additional analysis was conducted excluding the three participants with PDD-NOS diagnosis and their matched controls. The fMRI activation findings for the core ASD sample (eight high-functioning participants with Autistic disorder, three with Asperger's disorder) were highly similar, including robust clusters of activation in right lingual gyrus and right cuneus (areas 17, 18).

FcMRI analysis 1: Extrastriate seed

In order to characterize the connectivity of extrastriate cortex, an fcMRI analysis was performed using a seed in right cuneus, as detected in the activation analysis for the ASD group (see asterisk in Table 2). Both groups showed similar extensive connectivity between extrastriate cortex and posterior regions (Table 3; Fig. 1B). Direct between-group comparison revealed significantly greater fcMRI effects for the ASD group in anterior cingulate gyrus, medial frontal cortex, and lateral portions of middle and superior frontal gyri (Table 3; Fig. 1B).

FcMRI analysis 2: Left inferior frontal seed

The first fcMRI analysis revealed greater fcMRI effects in the ASD group between extrastriate cortex and frontal regions, which were largely located outside left inferior frontal gyrus. To further investigate potentially atypical connectivity between frontal and posterior brain regions in ASD, a second fcMRI analysis was conducted using a seed in LIFG derived from activation analyses performed for both groups pooled together (to avoid group bias in seed selection). The TD group showed functional connectivity of LIFG with homotopic right IFG, and left middle temporal, and angular gyri (Table 4; Fig. 1C). The ASD group showed more widespread fcMRI effects for LIFG across multiple regions. Direct group comparison showed greater fcMRI effects in the ASD group between LIFG and numerous brain regions, especially in left temporal and occipital lobes, with additional clusters in right frontal regions (Fig. 1C).

Potential confounds: Differences in head motion, performance, VIQ, and physiological noise

Additional analyses were performed to assess whether diffusely increased fcMRI effects in the ASD group could be attributed to excessive head motion. First, between-group differences in head motion were statistically analyzed by comparing the estimated maximum displacement between each acquired brain volume and the reference volume. The standard

deviation of maximum displacement across time provides an overall measure of each participant's head motion during scanning. Each group's standard deviation of maximum displacement was entered into a two-sample, two-tailed independent t-test. The difference in head motion between the two groups did not reach statistical significance (t_{26} = 1.90, p = .07).

Since marginally greater head motion in ASD participants could have nonetheless contributed to our findings (Auer, 2008), a second analysis was conducted, excluding three participants in the ASD group with greatest head motion and three TD participants with least head motion. An identical fcMRI analysis for the resulting subgroups (n=11 each), which were matched for motion (t_{20} = .48, p = .64), revealed overall similar results, with greater fcMRI effects across multiple brain regions in the ASD compared to the TD group for the LIFG seed (Suppl. Fig. 1). These group differences were thus unlikely to be explained by greater head motion in the ASD group. Motion parameters were also included as six orthogonal regressors in fcMRI analyses, which further reduced the likelihood of motion being a major confound in our findings.

In view of group difference in accuracy on the semantic decision task, we removed the 5 ASD participants with the lowest accuracy and the 5 TD participants with the highest accuracy. The remaining subsamples (n=9 per group) were matched on performance [ASD M(SD) = 85.6% (3.4); TD M(SD) = 86.4% (4.6); p=.70]. As seen in Supplementary Figure 2, group differences from the fcMRI analyses for both extrastriate and LIFG seeds were similar to those for the complete sample; in fact, for the LIFG seed effects of greater connectivity in the performance-matched ASD subsample were highly robust in temporal and parietal lobes bilaterally.

Furthermore, groups were not matched on verbal IQ. We therefore removed the 5 ASD participants with the lowest verbal IQ and the 5 TD participants with the highest verbal IQ to create matched subsamples [ASD M(SD) = 103.0 (9.1); TD M(SD) = 103.6 (6.7); p=.88]. Group differences for the subsamples were consistent with those for complete samples for both fcMRI seeds (Supplementary Figure 3).

Finally, since physiological (cardiac and respiratory) noise may confound fcMRI results, we conducted an fcMRI analysis using a regressor extracted from the lateral ventricles. We followed a similar procedure as Biswal et al. (2010) by first segmenting CSF from each participant's structural image using FAST in FSL (Zhang et al., 2001). The lateral ventricles were then defined from the resulting CSF image using Analyze software (Robb et al., 1989) to create a mask. The mean timeseries was extracted from the ventricular mask and entered as a nuisance regressor in the fcMRI analysis. This analysis revealed overall similar results with greater fcMRI effects across multiple brain regions in the ASD compared to the TD group for the LIFG seed (Suppl. Fig. 4).

Correlations with Task Performance

We correlated the strength of activity (in z' score) in the extrastriate ROI (see asterisk in Table 2) with the behavioral performance on the semantic decision task. The ASD group showed a significant negative correlation between extrastriate activity and number of errors, but not RT (ASD numbers of errors: r = -.58, p<.05; ASD mean RT: r = -.34, p=.23). The TD group had no significant relationship between strength of extrastriate activity and performance (TD number of errors: r = -.24, p=.48; TD mean RT: r = -.13, p=.7).

We further investigated whether functional connectivity between extrastriate cortex and LIFG was associated with task performance. For each individual, the strength of functional connectivity between ESC and LIFG was correlated with the number of errors and mean

response time. The ASD group showed a significant negative correlation between number of errors on the semantic decision task and ESC-LIFG functional connectivity (r = -0.62, p = 0.018; Fig. 2A). Furthermore, the ASD group showed a trend toward a significant negative correlation between response time and ESC-LIFG functional connectivity (r = -0.52, p = 0.057; Fig. 2B). The TD group did not show significant correlations between functional connectivity and accuracy (r = -0.38, p = 0.22) or response time (r = 0.21, p = 0.53).

Structural Equation Modeling

The optimal model of effective connectivity between the four ROIs implicated in semantic processing (left and right IFG, left middle temporal gyrus, and right extrastriate cortex) is presented for each group in Figure 4. The χ^2 statistic as a measure of *poorness* of model fit (de Marco et al., 2009) was appropriately non-significant for both the ASD model (χ^2 (4) = 1.23; p = 0.87) and TD model (χ^2 (4) = 1.44; p = 0.84). Additionally, the Parsimonious Fit Index (PFI), the population-based index RMSEA), and the incremental fit index CFI all indicated a good statistical model fit for the ASD model (PFI = .99, RMSEA = 0, CFI = 1) and the TD model (PFI = .99, RMSEA = 0, CFI = 1). The optimal group model was then applied on a single subject level to test individual model fit. The majority of participants (TD n=10; ASD n=9) showed satisfactory individual model fit with the respective group model (non-significant χ^2). Mean path coefficients of this subsample of participants were largely consistent with those for complete samples (Figure 3). One sample *t*-tests showed that all mean path coefficients were significantly different from zero (see Supplementary Table 1).

Discussion

The current study was prompted by an earlier finding of atypical activity in extrastriate visual cortex in ASD for semantic decision (Gaffrey et al., 2007), in the context of similar findings from other studies using different verbal and nonverbal paradigms (Groen et al., 2010; Kana et al., 2006; Koshino et al., 2005; Samson et al., 2011). Our goal was to further characterize the functional significance of extrastriate cortex, using fcMRI and SEM to examine the neurofunctional network underlying semantic organization in ASD. More specifically, we aimed to determine whether extrastriate activity is merely a reflection of local processing bias, which would be associated with limited connectivity to other regions; or conversely, whether extrastriate cortex cooperates with typical sites of lexical semantic activation (such as LIFG). Consistent with the fMRI findings of the previous study (Gaffrey et al., 2007), our extended ASD sample showed atypically increased activation in extrastriate cortex, probably reflecting a greater reliance on visual processing during lexical tasks. However, in contrast with this earlier study, we found strength of extrastriate activity to be positively correlated with performance accuracy in the ASD (but not the TD) group. Differences in findings likely relate to methodological differences; i.e., use of a smaller ROI reflecting peak extrastriate activity in the present study and use of a more sensitive measure of mean activity (as opposed to number of activated voxels in the study by Gaffrey et al.).

Our first fcMRI analysis, which used the main extrastriate activation cluster as the seed ROI, revealed extensive functional connectivity for extrastriate cortex in the ASD group, suggesting that extrastriate cortex was not functioning in isolation. In fact, the ASD group showed significantly greater functional connectivity between extrastriate cortex and frontal areas. This finding is consistent with a recent EEG coherence study reporting atypically increased connectivity between occipital and frontal sites in young adults with ASD (Léveillé et al., 2010).

While in the ASD group functional connectivity of ESC was extensive in frontal regions, it was mostly seen outside LIFG. We therefore conducted a second analysis to explore

whether LIFG (the main frontal activation site for semantic decision) is functionally connected with other parts of extrastriate cortex. FcMRI analysis 2 used a seed in LIFG derived from pooled activation analysis in both groups. The TD group showed relatively distinct region-specific functional connectivity between LIFG and homotopic right IFG, left middle temporal gyrus, and left angular gyrus, consistent with previous fcMRI findings of a semantic network in healthy adults (Hampson et al., 2002). In the ASD group, however, fcMRI effects for LIFG were diffusely distributed across multiple regions in all four lobes, including extensive clusters in temporo-occipital extrastriate cortex. Taken together, our findings from activation analysis and fcMRI analysis 2 suggest that language networks are less distinctly organized in ASD than in typical development.

Atypical language participation of extrastriate regions may in turn prompt atypical recruitment of prefrontal cortex (as suggested by analysis 1), i.e., top-down mechanisms that may be compensatory in nature. Indeed, strength of functional connectivity between ESC and LIFG was correlated with task performance (i.e. greater accuracy and faster response) in the ASD, but not the TD group. Atypically enhanced participation of frontal areas in ASD was observed in a study of visual search (Keehn et al., 2008), possibly suggesting top-down control of visual attention. This may also be supported by atypical prefrontal activation (BAs 9, 44, and 46) detected in a recent meta-analysis of studies using visual word presentation in ASD (Samson et al., 2011). The findings of our fcMRI analysis 1 may thus reflect greater reliance on visual perceptual processing associated with more effortful top-down control during semantic processing in ASD.

For further interpretation of semantic network participation by perisylvian and extrastriate regions, we examined effective connectivity using structural equation modeling. SEM was originally applied in neuroimaging to infer the causality of known connectivity between brain regions (Büchel, 1997; Mechelli et al., 2002; Toni, 2002), has recently been extended to more exploratory analyses of networks with as yet unestablished connectivity (Alvarez et al., 2008; James et al., 2009; Zhuang et al., 2005; Zhuang et al., 2008). We chose a procedure to search for the optimal model in each group for four ROIs: left and right IFG, left middle temporal gyrus (MTG) and right extrastriate cortex (RESC). In the TD model, RIFG and LIFG turned out to be mutually interconnected core regions from which almost all connections within the network originated. Conversely, RESC played a marginal role within the TD model, as it did not influence any other ROI (McIntosh and Gonzalez-Lima, 1994). In the ASD group, the optimal model yielded no core ROI (or “hub”), but instead a serial and circular pathway between the four ROIs. Strong reciprocal connection between RESC and LIFG in the ASD model suggests an atypically enhanced network participation of extrastriate cortex via a direct path connecting it with inferior frontal cortex. This greater reliance on extrastriate cortex may relate to findings of partially enhanced visual-perceptual processing in ASD (Dakin and Frith, 2005; Kana et al., 2006; Koshino et al., 2005; Samson et al., 2011; Simmons et al., 2009), also supported by several fMRI studies (Keehn et al., 2008; Sahyoun et al., 2009; Soulières et al., 2009). In summary, the effective connectivity results are consistent with the findings from our functional connectivity analyses and suggest that network organization of semantic processing in ASD involves an atypical fronto-occipital loop.

Heavy reliance on visual cortex during semantic processing in ASD was thus supported by activation, fcMRI, and SEM results. While in TD children such reliance on visual cortex may reflect inefficiency and immature organization of semantic networks (Brown et al., 2005), atypically increased connectivity between frontal and extrastriate regions in tandem with enhanced activity within extrastriate cortex could suggest compensatory mechanisms in ASD, as supported by positive correlations with performance. However, developmental causality remains uncertain. For example, a recent EEG study in toddlers with ASD

suggested that impaired face perception may be secondary to enhanced processing of high spatial frequencies in the visual domain (Vlamings et al., 2010), generally consistent with a causal role of enhanced perceptual functioning in ASD (Mottron et al., 2006). Analogously, strong participation of visual cortices could be interpreted as an early neurofunctional characteristic in ASD affecting atypical semantic development from early on, rather than reflecting a relatively late-onset compensatory response.

Overly diffuse and disorganized functional connectivity in ASD, as suggested by our fcMRI results, could be related to impaired behavioral development coinciding with early brain growth abnormalities (Courchesne et al., 2001). Typical postnatal brain development is dependent on experiential effects, which drive the pruning of early synaptic connections and the retraction of axons, resulting in more efficient neural network connectivity (Gottlieb and Halpern, 2002; Kandel et al., 2000; Luo and O'Leary, 2005). Environmental input and stimulation promote functional brain development during early sensitive periods of development in the first few years of life (Black et al., 1998). Synaptic connections are retained and stabilized through activity (specifically synchronous firing of pre- and postsynaptic neurons). Lack of stimulus input during this sensitive period of neural plasticity will lead to profound alterations in brain organization, resulting in atypical behavioral development (Black et al., 1998; Greenough et al., 1987). In particular, social and communicative behaviors are a critical source of experiential input necessary for typical brain development (Mundy and Burnette, 2005). Children with ASD, however, have reduced eye contact (Chawarska and Volkmar, 2005), impaired joint attention and social orienting (Mundy and Burnette, 2005), fewer interactions with others (Carter et al., 2005), and less opportunity to develop pragmatic language (Tager-Flusberg et al., 2005). These impairments may affect both constructive mechanisms, such as synaptic stabilization and myelination, and regressive mechanisms, such as synaptic pruning and axon retraction. Evidence consistent with reduced synaptic pruning was found in a recent postmortem study showing increased density of dendritic spines in frontal, temporal, and parietal association cortices in ASD (Hutsler and Zhang, 2010).

Atypical early experience, leading to a disturbance of synaptic pruning and occurring at the same time as anatomical overgrowth, would result in disorganized connectivity in early childhood and beyond. One diffusion tensor imaging (DTI) study in small children with autism (ages 1.5–5.8 years) showed increased fractional anisotropy (FA), a marker of white matter integrity (Weinstein et al., 2011). This contrasts with DTI studies in older children, adolescents, and adults that have reported reduced FA across multiple brain regions (Alexander et al., 2007; Keller et al., 2007; Shukla et al., 2011). Our findings of partial functional overconnectivity in ASD may appear inconsistent with these latter DTI reports. However, DTI and fcMRI are sensitive to abnormalities of connectivity in very different ways. Whereas reduced FA in DTI may reflect the presence of axons with reduced directional coherence, the existence of such axons may be associated with diffusely increased BOLD signal coherence in fcMRI. Although DTI evidence of increased FA for the early childhood period of white matter overgrowth in ASD remains limited, our finding of diffuse functional overconnectivity may reflect the atypical survival of connections established during this period of overgrowth. As recently suggested by (Shih et al., 2011), functional overconnectivity in ASD may be linked to reduced local functional differentiation, resulting in an impairment of distinctly organized and specialized functional networks.

Our findings of diffusely increased fcMRI in ASD effects may appear inconsistent with previous reports of reduced functional connectivity in networks for sentence comprehension (Just et al., 2004), inhibitory control (Kana et al., 2007), problem solving (Just et al., 2007), and theory of mind (Kana et al., 2008; Mason et al., 2008), including the specific proposal of

reduced fronto-posterior connectivity (Schipul et al., 2011). Divergent findings may be attributed to methodological differences (Müller et al., 2011). Since task-related activation effects tend to correlate throughout activated brain regions, differences in functional connectivity between ASD and TD groups reported in these studies may largely reflect differences of activation profiles, particularly since correlation analyses were often limited to ROIs determined by activation results.

For the current study, we therefore chose fcMRI methods focusing on intrinsic BOLD fluctuations, using a low-pass filter and orthogonal regressors to remove task effects. Such an approach was preferred, as it promises to yield results that are maximally orthogonal to (already known) activation effects, reflecting intrinsic connectivity and interregional cooperation, rather than task-related activity. The utility of this intrinsic fcMRI approach has been shown in many studies detecting robust BOLD signal correlations in motor (Biswal et al., 1995), visual and auditory (Cordes et al., 2000), attention (Fox et al., 2006), episodic memory (Vincent et al., 2006), and language (Cordes et al., 2000; Hampson et al., 2002) networks. Importantly, phase-locked low-frequency oscillations within functional networks exist in task-related BOLD time series from fMRI activation studies and can be isolated through statistical removal of task effects (Fair et al., 2007; Fox and Raichle, 2007), as in the current study. Some previous fcMRI studies of ASD that similarly focused on intrinsic low-frequency BOLD fluctuations yielded mixed patterns of over- and under-connectivity (Agam et al., 2010; Ebisch et al., 2010; Monk et al., 2009; Turner et al., 2006; Welchew et al., 2005) or predominant overconnectivity (Mizuno et al., 2006; Noonan et al., 2009; Shih et al., 2010, 2011), consistent with our findings.

Functional connectivity MRI is extremely sensitive to artifacts related to head motion and physiological noise (stemming from heart beat and respiration; Power et al., 2011; Van Dijk et al., 2012). Although our processing pipeline included six head motion nuisance regressors to minimize such artifacts, we performed an additional analysis for motion-matched subsamples, as well as an analysis including a nuisance regressor extracted from the lateral ventricles (Supplementary Figures 1 and 4). Results for both analyses were largely consistent with those described above, although group differences for the extrastriate seed were less robust and did not survive cluster correction. While this may be related to reduced sample size on the secondary analysis for motion-matched subgroups, the use of an orthogonal regressor extracted from the entire lateral ventricles, following a procedure by Biswal et al. (2010), may do slightly more than remove physiological noise. Given the relatively low spatial resolution of functional images, partial volume effects from neighboring brain tissue, in particular caudate nuclei, cannot be entirely ruled out. Subtle effects of true BOLD signal fluctuations on time series extracted from the lateral ventricles could have contributed to the reduction of effects seen for the extrastriate seed. On the other hand, the finding of diffuse overconnectivity in the ASD group for the seed in left inferior frontal cortex was replicated in these secondary analyses, showing that overall our findings were unlikely to be driven by head motion or physiological noise.

Since our study used a block design with sequential (non-interleaved) slice acquisition, we did not perform slice time correction. A recent study by Sladky et al. (2011) showed that slice time correction improves the detection of activation effects in event-related designs and block designs with short block length (10 s in the cited study). Although our study used much longer blocks (31.2 s in the experimental, 20.8 s in the control condition), it cannot be ruled out that lack of slice time correction may have had subtle effects on activation findings. Note that for all fcMRI analyses in the present study data were low-pass filtered ($f < 0.1$ Hz), and results were therefore unlikely to be impacted by relatively small differences in slice acquisition time. Furthermore, given that acquisition and data processing protocols

were identical for both groups, it appears improbable that slice timing would have affected the regional patterns of between-group effects in either activation or fcMRI analyses.

In conclusion, individuals with ASD show unusual activation for semantic tasks in extrastriate cortex, suggesting atypical reliance on visual processing. Our fcMRI and SEM analyses indicate that extrastriate cortex does not function in isolation (as might be implied by models of local processing bias in autism), but is characterized by atypically increased functional and effective connectivity with frontal regions. Results from a second fcMRI analysis for a seed in LIFG suggest that language networks are characterized by abnormally diffuse connectivity in ASD, contrasting with more distinct connectivity patterns in the TD brain. This overall pattern of findings reflects neither general underconnectivity nor overconnectivity, but disorganized connectivity for language in ASD. This disordered connectivity, although detected in adolescence and adulthood, may be a result of early disturbances associated with the dual impact of brain growth anomalies and atypical experiential effects on the differentiation of functional networks.

Supplementary Material

Refer to Web version on PubMed Central for supplementary material.

Acknowledgments

This study was supported by the National Institutes of Health, R01-DC006155 and R01-MH081023, with additional funding from the National Institute on Deafness and Other Communicative Disorders, NIDCD 1T32 DC007361-03 (author BK). Special thanks to the participants and families who participated and to Frank Haist, Gang Chen, Wesley Thompson, Ben McKenna, and Aaron Lee for their help and insight on fcMRI and SEM analysis.

Abbreviations

ASD	autism spectrum disorder
LIFG	left inferior frontal gyrus
RESC	right extrastriate cortex
MTG	middle temporal gyrus

References

Agam Y, Joseph RM, Barton JJ, Manoach DS. Reduced cognitive control of response inhibition by the anterior cingulate cortex in autism spectrum disorders. Neuroimage. 2010; 52:336–347. [PubMed: 20394829]

Alexander AL, Lee JE, Lazar M, Boudos R, Dubray MB, Oakes TR, Miller JN, Lu J, Jeong EK, McMahon WM, Bigler ED, Lainhart JE. Diffusion tensor imaging of the corpus callosum in Autism. Neuroimage. 2007; 34:61–73. [PubMed: 17023185]

Alvarez RP, Biggs A, Chen G, Pine DS, Grillon C. Contextual fear conditioning in humans: cortical-hippocampal and amygdala contributions. J Neurosci. 2008; 28:6211–6219. [PubMed: 18550763]

American Psychiatric Association. Diagnostic and Statistical Manual of Mental Disorders - IV - TR. 4th ed.. American Psychiatric Association; Washington, DC.: 2000.

Auer DP. Spontaneous low-frequency blood oxygenation level-dependent fluctuations and functional connectivity analysis of the ‘resting’ brain. Magn Reson Imaging. 2008; 26:1055–1064. [PubMed: 18657923]

Beckmann CF, DeLuca M, Devlin JT, Smith SM. Investigations into resting-state connectivity using independent component analysis. Philosophical Transactions of the Royal Society of London. Series B: Biological Sciences. 2005; 360:1001–1013.

Bentler PM. Comparative fit indexes in structural models. Psychological Bulletin. 1990; 107(2):238–46. [PubMed: 2320703]

Biswal B, Yetkin FZ, Haughton VM, Hyde JS. Functional connectivity in the motor cortex of resting human brain using echo-planar MRI. Magn Reson Med. 1995; 34:537–541. [PubMed: 8524021]

Biswal BB, Mennes M, Zuo XN, Gohel S, Kelly C, Smith SM, Milham MP. Toward discovery science of human brain function. Proc Natl Acad Sci USA. 2010; 107(10):4734–9. [PubMed: 20176931]

Black, J.; Jones, T.; Nelson, C.; Greenough, W. Neuronal plasticity and the developing brain.. In: Alessi, N., editor. Handbook of child and adolescent psychiatry: Vol. 4. Varieties of development. Wiley; New York: 1998. p. 31-53.

Boucher J. Research Review: Structural language in autistic spectrum disorder - characteristics and causes. J Child Psychol Psychiatry. 2012; 53:219–233. [PubMed: 22188468]

Browne, MW.; Cudeck, R. Alternative ways of assessing model fit.. In: Bollen, KA.; Long, JS., editors. Testing structural equation models. Sage Publications; Newbury Park: 1993. p. 136-62.

Brown TT, Lugar HM, Coalson RS, Miezin FM, Petersen SE, Schlaggar BL. Developmental Changes in Human Cerebral Functional Organization for Word Generation. Cereb Cortex. 2005; 15:275–290. [PubMed: 15297366]

Büchel C, Friston KJ. Modulation of connectivity in visual pathways by attention: cortical interactions evaluated with structural equation modelling and fMRI. Cerebral Cortex. 1997; 7:768–778. [PubMed: 9408041]

Bullmore E, Horwitz B, Honey G, Brammer M, Williams S, Sharma T. How good is good enough in path analysis of fMRI data? Neuroimage. 2000; 11:289–301. [PubMed: 10725185]

Bullmore E, Sporns O. Complex brain networks: graph theoretical analysis of structural and functional systems. Nat Rev Neurosci. 2009; 10:186–198. [PubMed: 19190637]

Carter, A.; Davis, N.; Klin, A.; Volkmar, F. Social Development in Autism.. In: Volkmar, F.; Paul, R.; Klin, A.; Cohen, D., editors. Handbook of Autism and Pervasive Developmental Disorders. John Wiley & Sons; Hoboken, NJ: 2005. p. 312-334.

Chaminade T, Fonlupt P. Changes of effective connectivity between the lateral and medial parts of the prefrontal cortex during a visual task. European Journal of Neuroscience. 2003; 18:675–679. [PubMed: 12911763]

Chawarska, K.; Volkmar, F. Autism in Infancy and Early Childhood.. In: Volkmar, F.; Paul, R.; Klin, A.; Cohen, D., editors. Handbook of Autism and Pervasive Developmental Disorders. John Wiley & Sons; Hoboken, NJ: 2005. p. 223-246.

Chen, G.; Glen, DR.; Stein, JL.; Meyer-Lindenberg, AS.; Saad, ZS.; Cox, RW. Model Validation and Automated Search in FMRI Path Analysis: A Fast Open-Source Tool for Structural Equation Modeling.. Human Brain Mapping Conference; Chicago. 2007.

Cordes D, Haughton VM, Arfanakis K, Carew JD, Turski PA, Moritz CH, Quigley MA, Meyerand ME. Frequencies contributing to functional connectivity in the cerebral cortex in “resting-state” data. AJNR. American Journal of Neuroradiology. 2001; 22:1326–1333. [PubMed: 11498421]

Cordes D, Haughton VM, Arfanakis K, Wendt GJ, Turski PA, Moritz CH, Quigley MA, Meyerand ME. Mapping functionally related regions of brain with functional connectivity MR imaging. AJNR. American Journal of Neuroradiology. 2000; 21:1636–1644. [PubMed: 11039342]

Courchesne E, Karns CM, Davis HR, Ziccardi R, Carper RA, Tigue ZD, Chisum HJ, Moses P, Pierce K, Lord C, Lincoln AJ, Pizzo S, Schreibman L, Haas RH, Akshoomoff NA, Courchesne RY. Unusual brain growth patterns in early life in patients with autistic disorder: an MRI study. Neurology. 2001; 57:245–254. [PubMed: 11468308]

Dakin S, Frith U. Vagaries of visual perception in autism. Neuron. 2005; 48:497–507. [PubMed: 16269366]

de Marco G, Vrignaud P, Destrieux C, de Marco D, Testelin S, Devauchelle B, et al. Principle of structural equation modeling for exploring functional interactivity within a putative network of interconnected brain areas. Magnetic Resonance Imaging. 2009; 27:1–12. [PubMed: 18584986]

Dunn M, Gomes H, Sebastian MJ. Prototypicality of responses of autistic, language disordered, and normal children in a word fluency task. Child Neuropsychology. 1996; 2:99–108.

Ebisch SJ, Gallese V, Willems RM, Mantini D, Groen WB, Romani GL, Buitelaar JK, Bekkering H. Altered intrinsic functional connectivity of anterior and posterior insula regions in high-functioning participants with autism spectrum disorder. Hum Brain Mapp. 2010

Fair DA, Schlaggar BL, Cohen AL, Miezin FM, Dosenbach NU, Wenger KK, Fox MD, Snyder AZ, Raichle ME, Petersen SE. A method for using blocked and event-related fMRI data to study "resting state" functional connectivity. Neuroimage. 2007; 35:396–405. [PubMed: 17239622]

Forman SD, Cohen JD, Fitzgerald M, Eddy WF, Mintun MA, Noll DC. Improved assessment of significant activation in functional magnetic resonance imaging (fMRI): use of a cluster-size threshold. Magn Reson Med. 1995; 33:636–647. [PubMed: 7596267]

Fox MD, Corbetta M, Snyder AZ, Vincent JL, Raichle ME. Spontaneous neuronal activity distinguishes human dorsal and ventral attention systems. Proc Natl Acad Sci U S A. 2006; 103:10046–10051. [PubMed: 16788060]

Fox MD, Raichle ME. Spontaneous fluctuations in brain activity observed with functional magnetic resonance imaging. Nat Rev Neurosci. 2007; 8:700–711. [PubMed: 17704812]

Gaffrey MS, Kleinhans NM, Haist F, Akshoomoff N, Campbell A, Courchesne E, Müller R-A. Atypical [corrected] participation of visual cortex during word processing in autism: an fMRI study of semantic decision. Neuropsychologia. 2007; 45:1672–1684. [PubMed: 17336346]

Gonçalves MS, Hall DA, Johnsrude IS, Haggard MP. Can meaningful effective connectivities be obtained between auditory cortical regions? Neuroimage. 2001; 14:1353–1360. [PubMed: 11707091]

Gottlieb G, Halpern CT. A relational view of causality in normal and abnormal development. Dev Psychopathol. 2002; 14:421–435. [PubMed: 12349867]

Greenough WT, Black JE, Wallace CS. Experience and brain development. Child Development. 1987:539–559. [PubMed: 3038480]

Groen WB, Zwiers MP, van der Gaag RJ, Buitelaar JK. The phenotype and neural correlates of language in autism: An integrative review. Neurosci Biobehav Rev. 2008; 8:1416–25. [PubMed: 18562003]

Groen WB, Tesink C, Petersson KM, van Berkum J, van der Gaag RJ, Hagoort P, Buitelaar JK. Semantic, factual, and social language comprehension in adolescents with autism: an FMRI study. Cereb Cortex. 2010; 20:1937–1945. [PubMed: 20016003]

Hampson M, Peterson BS, Skudlarski P, Gatenby JC, Gore JC. Detection of functional connectivity using temporal correlations in MR images. Hum Brain Mapp. 2002; 15:247–262. [PubMed: 11835612]

Holmes, A.; Poline, JB.; Friston, KJ. Characterizing brain images with the general linear model.. In: Frackowiak, RSJ.; Friston, KJ.; Frith, CD.; Dolan, RJ.; Mazziotta, JC., editors. Human Brain Function. Academic Press; San Diego: 1997. p. 59-84.

Honey CJ, Sporns O, Cammoun L, Gigandet X, Thiran JP, Meuli R, Hagmann P. Predicting human resting-state functional connectivity from structural connectivity. Proc Natl Acad Sci U S A. 2009; 106:2035–2040. [PubMed: 19188601]

Hutsler JJ, Zhang H. Increased dendritic spine densities on cortical projection neurons in autism spectrum disorders. Brain Res. 2010; 1309:83–94. [PubMed: 19896929]

James GA, Kelley ME, Craddock RC, Holtzheimer PE, Dunlop BW, Nemeroff CB, Mayberg HS, Hu XP. Exploratory structural equation modeling of resting-state fMRI: applicability of group models to individual subjects. Neuroimage. 2009; 45:778–787. [PubMed: 19162206]

Jiang T, He Y, Zang Y, Weng X. Modulation of functional connectivity during the resting state and the motor task. Hum Brain Mapp. 2004; 22:63–71. [PubMed: 15083527]

Just MA, Cherkassky VL, Keller TA, Kana RK, Minshew NJ. Functional and anatomical cortical underconnectivity in autism: evidence from an FMRI study of an executive function task and corpus callosum morphometry. Cereb Cortex. 2007; 17:951–961. [PubMed: 16772313]

Just MA, Cherkassky VL, Keller TA, Minshew NJ. Cortical activation and synchronization during sentence comprehension in high-functioning autism: evidence of underconnectivity. Brain. 2004; 127:1811–1821. [PubMed: 15215213]

Kamio Y, Robins D, Kelley E, Swainson B, Fein D. Atypical lexical/semantic processing in high-functioning autism spectrum disorders without early language delay. J Autism Dev Disord. 2007; 37:1116–1122. [PubMed: 17080275]

Kamio Y, Toichi M. Dual Access to Semantics in Autism: Is Pictorial Access Superior to Verbal Access? Journal of Child Psychology and Psychiatry. 2000; 41:859–867. [PubMed: 11079428]

Kana RK, Keller TA, Cherkassky VL, Minshew NJ, Adam Just M. Atypical frontal-posterior synchronization of Theory of Mind regions in autism during mental state attribution. Soc Neurosci. 2008:1–18. [PubMed: 18633851]

Kana RK, Keller TA, Cherkassky VL, Minshew NJ, Just MA. Sentence comprehension in autism: thinking in pictures with decreased functional connectivity. Brain. 2006; 129:2484–2493. [PubMed: 16835247]

Kana RK, Keller TA, Minshew NJ, Just MA. Inhibitory control in high-functioning autism: decreased activation and underconnectivity in inhibition networks. Biol Psychiatry. 2007; 62:198–206. [PubMed: 17137558]

Kandel, ER.; Jessell, TM.; Sanes, JR. Sensory experience and the fine tuning of synaptic connections.. In: Kandel, ER.; Schwartz, JH.; Jessell, TM., editors. Principles of Neural Science. Elsevier; New York: 2000. p. 1115-1130.

Keehn B, Brenner L, Palmer E, Lincoln AJ, Müller R-A. Functional brain organization for visual search in ASD. Journal of the International Neuropsychological Society. 2008; 14:990–1003. [PubMed: 18954479]

Keller TA, Kana RK, Just MA. A developmental study of the structural integrity of white matter in autism. Neuroreport. 2007; 18:23–27. [PubMed: 17259855]

Knaus TA, Silver AM, Lindgren KA, Hadjikhani N, Tager-Flusberg H. fMRI activation during a language task in adolescents with ASD. Journal of the International Neuropsychological Society. 2008; 14:967–979. [PubMed: 18954477]

Koshino H, Carpenter PA, Minshew NJ, Cherkassky VL, Keller TA, Just MA. Functional connectivity in an fMRI working memory task in high-functioning autism. Neuroimage. 2005; 24:810–821. [PubMed: 15652316]

Léveillé C, Barbeau EB, Bolduc C, Limoges E, Berthiaume C, Chevrier E, Mottron L, Godbout R. Enhanced connectivity between visual cortex and other regions of the brain in autism: a REM sleep EEG coherence study. Autism Res. 2010; 3:280–285. [PubMed: 20717953]

Lord C, Risi S, Lambrecht L, Cook EH, Leventhal BL, DiLavore PC, Pickles A, Rutter M. The Autism Diagnostic Observation Schedule-Generic: A Standard Measure of Social and Communication Deficits Associated with the Spectrum of Autism. Journal of Autism and Developmental Disorders. 2000; 30:205–223. [PubMed: 11055457]

Lord, C.; Risi, S.; Pickels, A. Trajectory of language development in autistic spectrum disorders.. In: Rice, M.; Warren, S., editors. Developmental Language Disorders: From Phenotypes to Etiologies. Erlbaum; Mahwah (NJ): 2004. p. 7-29.

Lord C, Rutter M, Couteur A. Autism Diagnostic Interview-Revised: A revised version of a diagnostic interview for caregivers of individuals with possible pervasive developmental disorders. Journal of Autism and Developmental Disorders. 1994; 24:659–685. [PubMed: 7814313]

Luo L, O'Leary DD. Axon retraction and degeneration in development and disease. Annual Review of Neuroscience. 2005; 28:127–156.

Mason RA, Williams DL, Kana RK, Minshew N, Just MA. Theory of Mind disruption and recruitment of the right hemisphere during narrative comprehension in autism. Neuropsychologia. 2008; 46:269–280. [PubMed: 17869314]

McIntosh AR, Gonzalez-Lima F. Structural Equation Modeling and Its Application to Network Analysis in Functional Brain Imaging. Human Brain Mapping. 1994; 2:2–22.

Mechelli A, Penny WD, Price CJ, Gitelman DR, Friston KJ. Effective connectivity and intersubject variability: using a multisubject network to test differences and commonalities. Neuroimage. 2002; 17:1459–1469. [PubMed: 12414285]

Mizuno A, Villalobos ME, Davies MM, Dahl BC, Müller R-A. Partially enhanced thalamo-cortical functional connectivity in autism. Brain Research. 2006; 1104:160–174. [PubMed: 16828063]

Monk CS, Peltier SJ, Wiggins JL, Weng SJ, Carrasco M, Risi S, Lord C. Abnormalities of intrinsic functional connectivity in autism spectrum disorders. Neuroimage. 2009; 47:764–772. [PubMed: 19409498]

Mottron L, Dawson M, Soulieres I, Hubert B, Burack J. Enhanced perceptual functioning in autism: an update, and eight principles of autistic perception. J Autism Dev Disord. 2006; 36:27–43. [PubMed: 16453071]

Müller R-A, Shih P, Keehn B, DeYoe J, Leyden KM, Shukla DK. Underconnected, but how? A survey of functional connectivity MRI studies in autism spectrum disorders. Cereb Cortex. 2011

Mundy, P.; Burnette, C. Handbook of Autism and Pervasive Developmental Disorders. John Wiley & Sons; Hoboken, NJ: 2005. Joint Attention and Neurodevelopmental Models of Autism.; p. 650-681.

Noonan SK, Haist F, Müller R-A. Aberrant functional connectivity in autism: Evidence from low-frequency BOLD signal fluctuations. Brain Research. 2009; 1262:48–63. [PubMed: 19401185]

Penny WD, Stephan KE, Mechelli A, Friston KJ. Modelling functional integration: a comparison of structural equation and dynamic causal models. Neuroimage. 2004; 23(Suppl 1):S264–274. [PubMed: 15501096]

Power JD, Barnes KA, Snyder AZ, Schlaggar BL, Petersen SE. Spurious but systematic correlations in functional connectivity MRI networks arise from subject motion. Neuroimage. 2011; 59:2142–54. [PubMed: 22019881]

Sahyoun CP, Soulieres I, Belliveau JW, Mottron L, Mody M. Cognitive differences in pictorial reasoning between high-functioning autism and Asperger's syndrome. J Autism Dev Disord. 2009; 39:1014–1023. [PubMed: 19267190]

Samson F, Mottron L, Soulieres I, Zeffiro TA. Enhanced visual functioning in autism: An ALE meta-analysis. Hum Brain Mapp. 2011

Schipul SE, Keller TA, Just MA. Inter-regional brain communication and its disturbance in autism. Front Syst Neurosci. 2011; 5:10. [PubMed: 21390284]

Robb RA, Hanson DP, Karwoski RA, Larson AG, Workman EL, Stacy MC. Analyze: A comprehensive, operator-interactive software package for multidimensional medical image display and analysis. Computerized Medical Imaging and Graphics. 1989; 13(6):433–454. [PubMed: 2688869]

Shih P, Keehn B, Oram JK, Leyden KM, Keown CL, Müller R-A. Functional Differentiation of Posterior Superior Temporal Sulcus in Autism: A Functional Connectivity Magnetic Resonance Imaging Study. Biol Psychiatry. 2011

Shih P, Shen M, Öttl B, Keehn B, Gaffrey MS, Müller R-A. Atypical network connectivity for imitation in autism spectrum disorder. Neuropsychologia. 2010; 48:2931–2939. [PubMed: 20558187]

Shukla DK, Keehn B, Muller RA. Tract-specific analyses of diffusion tensor imaging show widespread white matter compromise in autism spectrum disorder. J Child Psychol Psychiatry. 2011; 52:286–295. [PubMed: 21073464]

Simmons DR, Robertson AE, McKay LS, Toal E, McAleer P, Pollick FE. Vision in autism spectrum disorders. Vision Res. 2009; 49:2705–2739. [PubMed: 19682485]

Sladky R, Friston KJ, Trostl J, Cunnington R, Moser E, Windischberger C. Slice-timing effects and their correction in functional MRI. Neuroimage. 2011; 58:588–594. [PubMed: 21757015]

Soulières I, Dawson M, Samson F, Barbeau EB, Sahyoun CP, Strangman GE, Zeffiro TA, Mottron L. Enhanced visual processing contributes to matrix reasoning in autism. Hum Brain Mapp. 2009

Steiger JH. Structural model evaluation and modification: An interval estimation approach. Multivariate Behavioral Research. 1990; 25(2):173–180.

Tager-Flusberg, H.; Paul, R.; Lord, C. Language and communication in autism.. In: Volkmar, FR.; Paul, R.; Klin, A.; Cohen, D., editors. Handbook of Autism and Pervasive Developmental Disorders. Wiley; New York: 2005. p. 335-364.

Toichi M, Kamio Y. Verbal association for simple common words in high-functioning autism. J Autism Dev Disord. 2001; 31:483–490. [PubMed: 11794413]

Toni I, Rowe J, Stephan KE, Passingham RE. Changes of cortico-striatal effective connectivity during visuomotor learning. Cereb Cortex. 2002; 12:1040–1047. [PubMed: 12217967]

Turner KC, Frost L, Linsenbardt D, McIlroy JR, Müller R-A. Atypically diffuse functional connectivity between caudate nuclei and cerebral cortex in autism. Behavioral and Brain Functions. 2006; 2:34–45. [PubMed: 17042953]

Van Dijk KR, Hedden T, Venkataraman A, Evans KC, Lazar SW, Buckner RL. Intrinsic functional connectivity as a tool for human connectomics: theory, properties, and optimization. J Neurophysiol. 2010; 103:297–321. [PubMed: 19889849]

Van Dijk KR, Sabuncu MR, Buckner RL. The influence of head motion on intrinsic functional connectivity MRI. Neuroimage. 2012; 59:431–438. [PubMed: 21810475]

Vincent JL, Snyder AZ, Fox MD, Shannon BJ, Andrews JR, Raichle ME, Buckner RL. Coherent spontaneous activity identifies a hippocampal-parietal memory network. J Neurophysiol. 2006; 96:3517–3531. [PubMed: 16899645]

Vlamings PH, Jonkman LM, van Daalen E, van der Gaag RJ, Kemner C. Basic abnormalities in visual processing affect face processing at an early age in autism spectrum disorder. Biol Psychiatry. 2010; 68:1107–1113. [PubMed: 20728876]

Walenski M, Mostofsky SH, Gidley-Larson JC, Ullman MT. Brief report: enhanced picture naming in autism. J Autism Dev Disord. 2008; 38:1395–1399. [PubMed: 18163206]

Wechsler. Wechsler abbreviated scale of intelligence. San Antonio, TX: 1999.

Weinstein M, Ben-Sira L, Levy Y, Zachor DA, Ben Itzhak E, Artzi M, Tarrasch R, Eksteine PM, Hendler T, Ben Bashat D. Abnormal white matter integrity in young children with autism. Hum Brain Mapp. 2011; 32:534–543. [PubMed: 21391246]

Welchew DE, Ashwin C, Berkouk K, Salvador R, Suckling J, Baron-Cohen S, Bullmore E. Functional disconnectivity of the medial temporal lobe in Asperger's syndrome. Biol Psychiatry. 2005; 57:991–998. [PubMed: 15860339]

Zhang Y, Brady M, Smith S. Segmentation of brain MR images through a hidden markov random field model and the expectation-maximization algorithm. IEEE Transactions on Medical Imaging. 2001; 20(1):45–57. [PubMed: 11293691]

Zhuang J, LaConte S, Peltier S, Zhang K, Hu X. Connectivity exploration with structural equation modeling: an fMRI study of bimanual motor coordination. Neuroimage. 2005; 25:462–470. [PubMed: 15784425]

Zhuang J, Peltier S, He S, LaConte S, Hu X. Mapping the connectivity with structural equation modeling in an fMRI study of shape-from-motion task. Neuroimage. 2008; 42:799–806. [PubMed: 18599316]

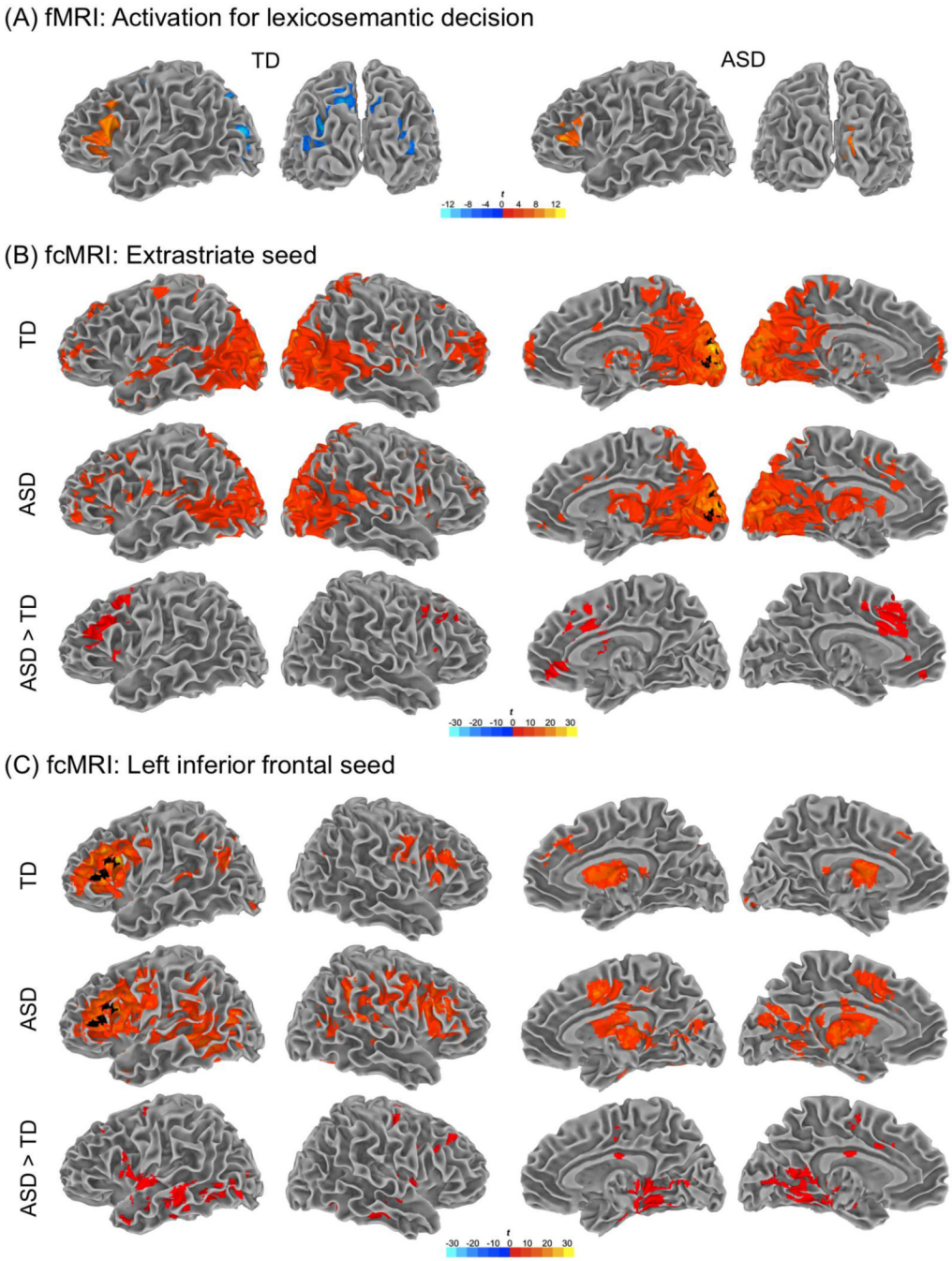

Figure 1.

(A) FMRI activation clusters for lexicosemantic decision (compared to letter detection control) in the TD and ASD groups. (B) Results for fcMRI analysis 1 (extrastriate seed): TD within-group effects, ASD within-group effects, ASD>TD between-group effects. (C) Results for fcMRI analysis 2 (LIFG seed): TD within-group effects, ASD within-group effects, ASD>TD between-group effects. Note: Seeds for each fcMRI analysis are shown in black; all clusters $p < .05$, corrected.

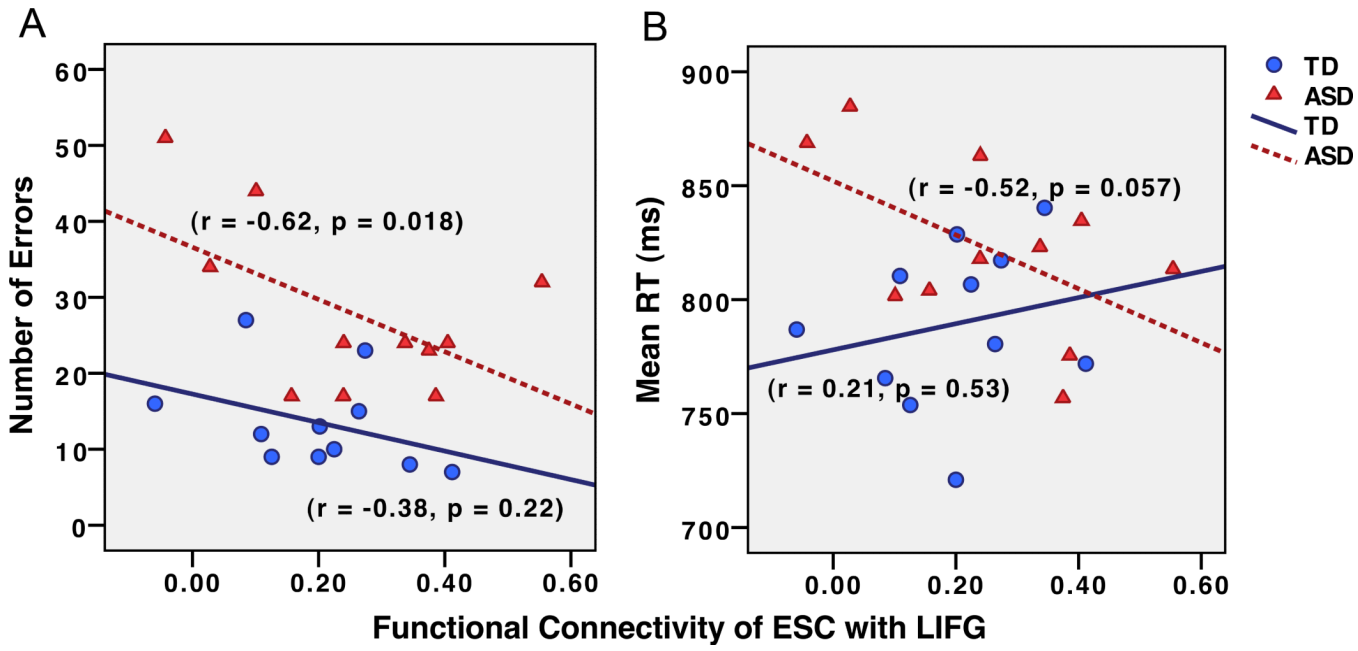

Figure 2.
Association between functional connectivity of ESC-LIFG (*r*) and (A) number of errors and (B) mean response time by group.

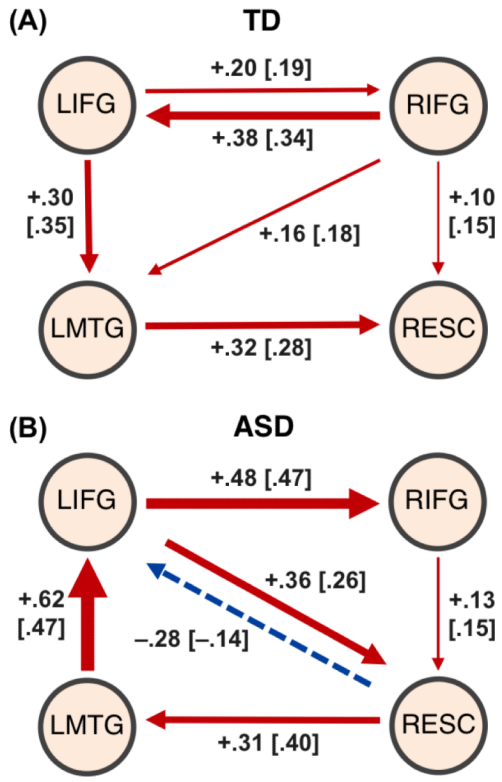

Figure 3.
Results of exploratory SEM analysis. Mean path coefficients of the model for semantic processing network, including left inferior frontal gyrus (LIFG), homotopic right inferior frontal gyrus (RIFG), left middle temporal gyrus (LMTG), and right extrastriate cortex (RESC), in TD and ASD groups. Models are shown separately for TD group (A) and ASD group (B). Line thickness reflects connection strength; red indicates positive connections, blue a negative connection. Path coefficients for subsamples of participants with non-significant χ^2 are shown in brackets.

Table 1

Participant Characteristics

	ASD (n = 14) M (SD) Range	TD (n = 14) M (SD) Range
Age	24.1 (9.5)	24.2 (8.4)
	15 - 44	14 - 42
NVIQ	107 (13.9)	114 (11.9)
	79 - 127	88 - 129
VIQ	93 (15.5)	110 (10.8)
	68 - 115	95 - 130
Handedness	11 R; 3 L	11 R; 3 L

M, mean; SD, standard deviation; NVIQ, nonverbal IQ; VIQ, verbal IQ; R, right; L, left.

Table 2

fMRI activation clusters for lexicosemantic decision task vs. control task. The asterisk indicates an extrastriate cluster used as seed in fcMRI analysis 1 and as ROI in correlation analyses.

	Peak location (Brodmann area) Additional regions (% volume of cluster)	Talairach coordinates x	y	z	Volume µl	t-value
TD group						
Activations	**L inferior frontal gyrus (44/45)**	-47	13	22	10184	8.1
	L inferior frontal gyrus (p. Triangularis) (69.1%)					
	L inferior frontal gyrus (p. Orbitalis) (14.2%)					
	L inferior frontal gyrus (p. Opercularis) (9.6%)					
	L middle frontal gyrus (2.1%)					
	L supplementary motor area (6)	-3	11	50	2224	7.5
	R cerebellum (VIII)	29	-61	-40	1096	7.1
	L calcarine cortex (17)	-9	-91	-8	888	7.7
	L caudate nucleus	-9	3	18	680	5.9
	R cerebellum (Crus 2)	17	-69	-36	432	6.5
Deactivations	**L precuneus (7)**	-13	-63	32	11960	-13.3
	L middle occipital gyrus (35.1%)					
	L precuneus (22.3%)					
	L superior parietal lobule (14.7%)					
	L superior occipital gyrus (12.0%)					
	R supramarginal gyrus (40)	55	-43	30	7896	-9.3
	R middle occipital gyrus (22.3%)					
	R supramarginal gyrus (15.9%)					
	R superior occipital gyrus (10.1%)					
	L middle cingulate cortex (31)	-9	-35	34	2952	-9.3
	L precentral gyrus (4)	-27	-15	44	952	-8.0
	R precentral gyrus (4)	29	-11	50	584	-6.1
	L middle frontal gyrus (9)	-25	33	34	488	-6.8
	L inferior occipital gyrus (18)	-47	-67	-6	472	-5.7
	L inferior parietal lobule (40)	-53	-43	36	416	-6.2

	Peak location (Brodmann area)					
	Additional regions (% volume of cluster)	Talairach coordinates			Volume	
		x	y	z	μl	t-value
ASD group						
Activations	**L inferior frontal gyrus (44/45)**	-45	33	10	3336	8.2
	R cuneus (17/18) *	13	-87	12	1824	7.2
	R lingual gyrus (18)	19	-71	-8	496	6.4
ASD > TD						
	L superior parietal lobule (7)	-13	-67	40	6800	4.5
	L precuneus (20.1%)					
	L cuneus (19.6%)					
	R superior occipital gyrus (15.1%)					
	L superior occipital gyrus (11.7%)					
	L superior parietal lobule (10.3%)					
	L middle occipital gyrus (9.8%)					
	R cuneus (7.7%)					
	L superior frontal gyrus (6)	-21	-7	48	2616	4.0

Table 3

FcMRI clusters for Analysis 1: Extrastriate seed ROI.

TD Group						ASD Group						Group comparison					
Peak location (Brodmann area)	**Talairach coordinates**			**Volume**		**Peak location (Brodmann area)**	**Talairach coordinates**			**Volume**		**Peak location (Brodmann area)**	**Talairach coordinates**			**Volume**	
Additional regions (% volume of cluster)	**x**	**y**	**z**	**μl**	**t-value**	**Additional regions (% volume of cluster)**	**x**	**y**	**z**	**μl**	**t-value**	**Additional regions (% volume of cluster)**	**x**	**y**	**z**	**μl**	**t-value**
R cuneus (17/18)	9	-87	16	298696	27.3	**R cuneus (17/18)**	5	-89	8	244080	26.5	**ASD > TD**					
L middle occipital gyrus (5.3%)						L middle occipital gyrus (5.6%)						**L middle cingulate cortex (24)**	-11	15	32	39960	4.1
L precuneus (4.5%)						L calcarine gyrus (4.4%)						L middle frontal gyrus (13.4%)					
R middle temporal gyrus (4.1%)						R lingual gyrus (4.1%)						L inferior frontal gyrus (10.1%)					
R precuneus (4.1 %)						R middle temporal gyrus (3.9%)						L superior medial gyrus (5.8%)					
L calcarine gyrus (3.9%)						R precuneus (3.8%)						L anterior cingulate cortex (5.3%)					
L lingual gyrus (3.5%)						L lingual gyrus (3.8%)						L superior frontal gyrus (3.9%)					
R lingual gyrus (3.4%)						R calcarine gyrus (3.5%)						R anterior cingulate cortex (3.7%)					
R middle occiptal gyrus (3.2%)						L middle temporal gyrus (3.4%)						R middle frontal gyrus (3.2%)					
R calcarine gyrus (2.9%)						R middle occipital gyrus (3.4%)						R mid orbital gyrus (3.0%)					
L cuneus (2.8%)						L cuneus (3.1%)						R middle cingluate cortex (2.7%)					
L middle temporal gyrus (2.8%)						R cuneus (2.9%)						R superior frontal gyrus (2.4%)					
R cuneus (2.6%)						L superior occipital gyrus (2.9%)						L insula lobe (2.2%)					
L cerebellum (Crus 1) (2.5%)						R cerebellum (Crus 1) (2.3%)						R putamen (2.0%)					
R cerebellum (Crus 1) (2.5%)						R cerebellum (VI) (2.3)											
L superior occipital gyrus (2.3%)						R superior occipital gyrus (2.3%)											
R superior occipital gyrus (2.0%)						L cerebellum (VI) (2.2%)											
R superior medial frontal gyrus (10)	13	59	12	30192	12.8	**L middle orbital gyrus (10)**	-29	49	-2	7944	8.1	**TD > ASD**					
R middle frontal gyrus (17.9%)						L middle frontal gyrus (53.2%)						No significant effects					

Neuroimage. Author manuscript; available in PMC 2013 December 10.

TD Group					
Peak location (Brodmann area)	**Talairach coordinates**			**Volume**	
Additional regions (% volume of cluster)	**x**	**y**	**z**	**μl**	**t-value**
L middle frontal gyrus (16.3%)					
R superior frontal gyrus (9.8%)					
R inferior frontal gyrus (p. Triangularis) (9.2%)					
L superior frontal gyrus (8.6%)					
R middle occipital gyrus (6.0%)					
R superior medial gyrus (5.7%)					
L middle orbital gyrus (4.5%)					
L superior medial gyrus (4.2%)					
L superior orbital gyrus (4.0%)					
L mid orbital gyrus (3.8%)					
R mid orbital grus (2.6%)					
L superior temporal gyrus (42)	-59	-19	10	6464	11.4
L superior frontal gyrus (66.6%)					
L middle temporal gyrus (21.4%)					
L middle temporal pole (4.5%)					
L caudate nucleus	-23	-5	28	1000	8.5
L postcentral gyrus (3)	-35	-19	30	872	8.0
R inferior frontal gyrus (p. Opercularis) (44)	31	1	34	824	8.4
L precentral gyrus (6)	-39	-19	52	744	10.3
L inferior temporal gyrus (21)	-53	-7	-22	664	9.6
R postcentral gyrus (3)	51	-9	28	656	8.1
R superior frontal gyrus (8)	19	19	36	448	7.4
R anterior cingulate cortex (24)	3	5	30	400	8.5
R cerebellum (VIII)	25	-37	-44	376	8.0
R insula lobe (13)	45	7	4	328	7.1

ASD Group					
Peak location (Brodmann area)	**Talairach coordinates**			**Volume**	
Additional regions (% volume of cluster)	**x**	**y**	**z**	**μl**	**t-value**
L inferior frontal gyrus (p. Triangularis) (23.6%)					
L middle orbital gyrus (12.1 %)					
L inferior frontal gyrus (p. Orbitalis) (4.1 %)					
L precentral gyrus (3.4%)					
L supplementary motor area (6)	-7	1	44	4080	7.7
R middle frontal gyrus (6)	25	3	46	3208	7.3
R superior frontal gyrus (10)	27	49	20	2544	8.2
L inferior frontal gyrus (p. Orbitalis) (47)	-43	19	-4	1680	9.7
R mid orbital gyrus (32)	15	35	2	800	8.5
R insula lobe (47)	43	17	-2	616	6.9
R precentral gyrus (6)	39	-5	42	280	6.8
L insula lobe (13)	-25	-49	8	160	6.6
R inferior frontal gyrus (p. Orbitalis) (47)	29	25	-14	144	7.2

Group comparison					
Peak location (Brodmann area)	**Talairach coordinates**			**Volume**	
Additional regions (% volume of cluster)	**x**	**y**	**z**	**μl**	**t-value**

TD Group						ASD Group						Group comparison					
Peak location (Brodmann area)	Talairach coordinates			Volume		Peak location (Brodmann area)	Talairach coordinates			Volume		Peak location (Brodmann area)	Talairach coordinates			Volume	
Additional regions (% volume of cluster)	x	y	z	μl	t-value	Additional regions (% volume of cluster)	x	y	z	μl	t-value	Additional regions (% volume of cluster)	x	y	z	μl	t-value
R cerebellum (III)	15	-23	-26	232	10.4												
R superior frontal gyrus (8)	21	25	44	232	8.4												
R inferior frontal gyrus (44)	59	7	18	224	7.3												
L medial temporal pole (38)	-49	11	-24	216	7.4												

Table 4

FcMRI clusters for Analysis 2: LIFG seed

TD Group						ASD Group						Group comparison					
Peak location (Brodmann area)	**Talairach coordinates**			**Volume**		**Peak location (Brodmann area)**	**Talairach coordinates**			**Volume**		**Peak location (Brodmann area)**	**Talairach coordinates**			**Volume**	
Additional regions (% volume of cluster)	**x**	**y**	**z**	**μl**	**t-value**	**Additional regions (% volume of cluster)**	**x**	**y**	**z**	**μl**	**t-value**	**Additional regions (% volume of cluster)**	**x**	**y**	**z**	**μl**	**t-value**
L inferior frontal gyrus (p. Triangularis) (44/45)	-51	15	22	53384	32.7	**L inferior frontal gyrus (p. Triangularis) (44/45)**	-45	23	22	231016	29.0	**ASD > TD**					
L inferior frontal gyrus (p. Triangularis) (24.9%)						L inferior frontal gyrus (p. Triangularis) (5.6%)						**L lingual gyrus (18)**	-5	-45	0	74040	5.6
L middle frontal gyrus (7.9%)						L middle temporal gyrus (4.7%)						L middle temporal gyrus (7.6%)					
L inferior frontal gyrus (p. Opercularis) (7.7%)						L precentral gyrus (3.3%)						R fusiform gyrus (4.9%)					
L precentral gyrus (7.3%)						R inferior frontal gyrus (p. Triangularis) (3.1%)						L inferior temporal gyrus (4.9%)					
L middle temporal gyrus (5.1%)						L middle occipital gyrus (2.6%)						L lingual gyrus (4.4%)					
L caudate nucleus (5.1%)						R inferior frontal gyrus (p. Opercularis) (2.5%)						L calcarine gyrus (3.1 %)					
L thalamus (4.2%)						R precentral gyrus (2.5%)						L hippocampus (3.0%)					
L insula lobe (4.2%)						L inferior frontal gyrus (p. Opercularis) (2.4%)						R inferior temporal gyrus (3.0%)					
L inferior frontal gyrus (p. Orbitalis) (3.7%)						L middle frontal gyrus (2.1%)						L fusiform gyrus (2.8%)					
R inferior frontal gyrus (p. Triangularis) (45)	41	23	28	10272	12.2	R cerebellum (Crus 1) (2.1%)						R lingual gyrus (2.8%)					
R inferior frontal gyrus (p. Triangularis) (34.8%)						L thalamus (2.1%)						R cerebellum IV-V (2.5%)					
R inferior frontal gyrus (p. Opercularis) (12.4%)						R thalamus (2.0%)						L insula lobe (2.2%)					
R precentral gyrus (9.3%)						**R calcarine gyrus (17)**	17	-59	4	856	9.8	L middle frontal gyrus (2.2%)					
R postcentral gyrus (9.3%)						**R fusiform gyrus (20)**	39	-17	-24	736	12.3	L precentral gyrus (2.1%)					
R insula lobe (6.9%)						**L cerebellum (Crus 1)**	-17	-71	-26	400	8.6	L putamen (2.1%)					
R middle frontal gyrus (3.8%)						**R superior temporal gyrus (22)**	43	-29	-2	296	9.7	**R precentral gyrus (4)**	31	-15	46	6192	4.7
R rolandic operculum (2.9%)						**L fusiform gyrus (20)**	-27	-1	-30	184	10.8	R superior frontal gyrus (25.5%)					
R cerebellum (VII)	35	-65	-44	7064	13.8	**L inferior temporal gyrus (21)**	-37	11	-32	112	8.7	R precentral gyrus (18.3%)					

TD Group						ASD Group						Group comparison					
Peak location (Brodmann area)	**Talairach coordinates**			**Volume**		**Peak location (Brodmann area)**	**Talairach coordinates**			**Volume**		**Peak location (Brodmann area)**	**Talairach coordinates**			**Volume**	
Additional regions (% volume of cluster)	**x**	**y**	**z**	**μl**	**t-value**	**Additional regions (% volume of cluster)**	**x**	**y**	**z**	**μl**	**t-value**	**Additional regions (% volume of cluster)**	**x**	**y**	**z**	**μl**	**t-value**
L middle temporal gyrus, angular gyrus (39)	-41	-65	24	3144	13.8	**L medial temporal pole (38)**	-47	7	-20	104	8.9	R SMA (10.9%)					
L anterior cingulate cortex (24)	-11	27	32	2040	10.7	**L lingual gyrus (17/18)**	-21	-67	-2	96	8.2	R middle cingulate cortex (4.9%)					
L cerebellum (VIII)	-33	-47	-38	1928	10.0	**R cerebellum (X)**	25	-33	-34	80	8.0	R middle frontal gyrus (3.3%)					
L superior occipital gyrus (19)	-25	-71	34	1320	9.7							**R middle frontal gyrus (9)**	31	27	36	1328	4.2
L superior temporal gyrus (22)	-61	-33	10	712	11.6												
R lingual gyrus (17/18)	15	-93	-10	450	10.4							**TD > ASD**					
L inferior occipital gyrus (18)	-21	-89	-10	384	8.6							No significant effects					
L inferior parietal lobule (40)	-45	-43	40	384	9.5												
L superior medial gyrus (9)	-3	43	20	128	8.2												